Synthesis and structure of a new bulky bis(alkoxide) ligand on a

terphenyl platform

Sudheer S. Kurup, a Sandra Nasser, a Cassandra L. Ward, b Stanislav Groysman

^aDepartment of Chemistry, Wayne State University, 5101 Cass Ave. Detroit MI 48202.

^bLumigen Instrument Center, Wayne State University, 5101 Cass Avenue, Detroit, Michigan

48202, United States.

E-mails: groysman@wayne.edu, lordri@gvsu.edu

Abstract

A new sterically bulky chelating bis(alkoxide) ligand 3,3'-([1,1':4',1"-terphenyl]-2,2"-

diyl)bis(2,2,4,4-tetramethylpentan-3-ol) (H₂[OO]^{tBu}) was prepared in a two step process. The

first step is a Suzuki-Miyaura coupling reaction between 2-bromophenylboronic acid and 1,4-

diiodobenzene. The resulting 2,2"-dibromo-1,1':4',1"-terphenyl was reacted with 'BuLi and

hexamethylacetone to obtain the desired product. The crystal structure of H₂[OO]^{tBu} revealed

anti conformation of [CPh₂(OH)] fragments relatively to the central phenyl. Furthermore, the

hydroxyl groups point away from each other. Likely due to this anti-anti conformation, the

attempts to synthesize first-row transition metal complexes with H₂[OO]^{tBu} were not successful.

1. Chemical context

Bulky alkoxides are becoming increasingly used as ancillary ligands in group-transfer chemistry and catalysis.(Brazeau & Doerrer, 2019; Chua & Duong, 2014; Hannigan et al., 2017; Jayasundara et al., 2018, Wannipurage et al., 2020) Due to their stereoelectronic properties, profoundly weak-field bulky alkoxides enable formation of reactive low-coordinate high-spin middle and late transition metal centers. (Bellow, Yousif & Groysman, 2016; Grass, Wannipurage et al., 2019) We have previously reported bulky monodentate alkoxides that led to reactive chromium and iron nitrene-transfer catalysts, (Bellow et al., 2015, Wannipurage et al., 2021, Yousif et al., 2015; Yousif et al., 2018) and a series of low-coordinate cobalt carbene complexes capable of carbene transfer to isocyanides. (Bellow, Stoian et al., 2016; Grass, Dewey et al., 2019, Grass et al., 2020) However, the lability of monodentate alkoxides affected catalyst stability and the substrate scope. To remediate the problem of lability of monodentate alkoxides, we have designed and synthesized a new chelating bis(alkoxide) ligand [1,1':4',1"-terphenyl]-2,2"-diylbis(diphenylmethanol) (H₂[OO]^{Ph}) (**Figure 1**).(Kurup *et al.*, 2019) H₂[OO]^{Ph} ligand employs 1,1':4',1"-terphenyl platform, which increases the bite angle between the alkoxide donors to form an approximately seesaw transition metal centers. While the isolated ligand precursor H₂[OO]^{Ph} exhibited anti conformation of the [CPh₂(OH)] fragments relatively to the central phenyl in the solid state (crystals obtained at -35 °C), the hydroxyls were pointing towards the central phenyl, exhibiting overall the "anti-syn" conformation (Figure 1).(Kurup et al., 2019) Furthermore, while two different isomers were observed by ¹H NMR spectroscopy at low temperatures, a single species was observed at room temperature, suggesting facile equilibration of anti and syn conformers. As a result, H₂[OO]^{Ph} led to the formation of the desired bis(alkoxide) complexes with iron and chromium (Figure 1).(Kurup et al., 2019; Kurup

et al., 2020) The resulting iron complex exhibited broader range of nitrene transfer reactivity, forming a variety of symmetric azoarenes.

Figure 1. Schematic representation of the "anti-syn" structure of previously synthesized $H_2[OO]^{Ph}$ ligand and its reactivity with transition metal precursors.

The success of this strategy led us to design a new, even bulkier ligand (H₂[OO]^{tBu}). The ligand was synthesized in a two-step procedure as described in Figure 2. Previously reported 2,2"-dibromo-1,1':4',1"-terphenyl was synthesized through Suzuki-Miyaura coupling reaction between 2-bromophenylboronic acid and 1,4-diiodobenzene following literature procedure.(Velian et al., 2010) Next, 2,2"-dibromo-1,1':4',1"-terphenyl was treated with 'BuLi followed by hexamethylacetone. The formation of the desired product H₂[OO]^{tBu} (35% isolated yield) was accompanied by the formation of significant amounts of p-terphenyl by-product (38%) isolated yield). H₂[OO]^{tBu} was characterized by ¹H and ¹³C NMR spectroscopy, high-resolution mass spectrometry, and X-ray crystallography. ¹H NMR spectroscopy demonstrates the presence of two isomers at room temperature in approximately 2:1 ratio, as manifested by two tert-butyl resonances (1.05 and 1.03 ppm) and two OH resonances (2.09 and 2.07 ppm). This observation suggests that, in contrast to H₂[OO]^{Ph}, various isomers of H₂[OO]^{tBu} do not readily interconvert at room temperature, possibly due to the more significant steric hindrance of tert-butyl groups. X-ray crystallography (see below) suggested that in at least one of these isomers the hydroxyl

groups are pointing away from each other; such an isomer is unlikely to coordinate a single metal in a chelating fashion. Accordingly, the reaction of $H_2[OO]^{tBu}$ with several representative transition metal amides (M = Cr, Mn, Fe) failed to produce isolable complexes.

Figure 2. Synthesis of $H_2[OO]^tBu$, its schematic structure, and the lack of well-defined reactivity with transition metal amide precursors.

2. Structural commentary

The crystals of $H_2[OO]^{tBu}$ were obtained from dichloromethane at -35 °C. The structure crystallized in point group P-1 and is presented in **Figure 3**. Selected bond distances and angles are given in **Table 1**. $H_2[OO]^{tBu}$ exhibits a crystallophic inversion center, with only half of the molecule occupying an asymmetric unit. In addition to $H_2[OO]^{tBu}$, the structure contains one solvent molecule (CH_2Cl_2) disordered by symmetry over two positions. Selected bond distances, angles, and torsion angles appear in **Table 1**. The lateral phenyls of the terphenyl unit are approximately perpendicular to the central phenyl, as indicated by the corresponding torsion angles close to 90 ° (see **Table 1**). Similar to the structure of $H_2[OO]^{Ph}$, $H_2[OO]^{tBu}$ manifests the *anti* conformation of the two " $[C^tBu_2(OH)]$ " donors relative to the central phenyl. In contrast to

the structure of $H_2[OO]^{Ph}$, the hydroxyls point away from each other in the structure of $H_2[OO]^{tBu}$, leading to the overall "anti-anti" conformation. This disposition results in the placement of tert-butyl groups above and below the central phenyl. The presence of bulky groups on both sides of the central phenyl is likely responsible for the distortion of the terphenyl fragment, that is indicated by the C10 C15 C16 angle of 130.70(15)° and the C14 C15 C16 angle of 110.28(15)°. Same distortion is likely responsible for the slight variation in (lateral) phenyl bond distances (Table 1).

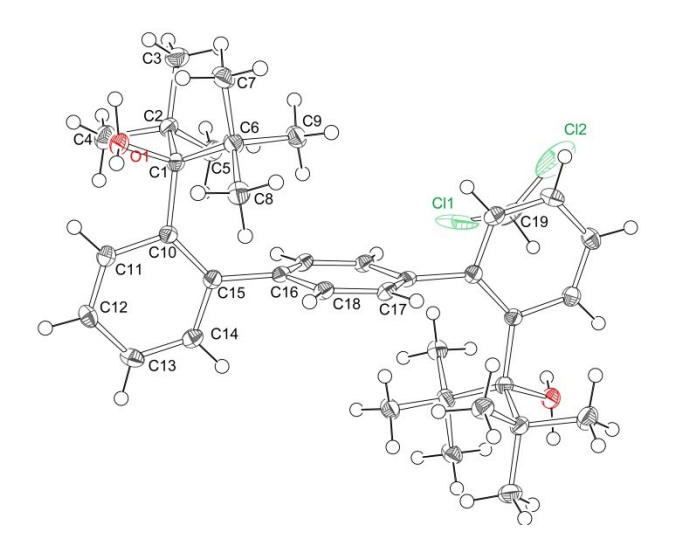


Figure 3. The structure of H₂[OO]^tBu (50% probability ellipsoids), shown with cocrystallized dichloromethane solvent molecule. The carbon of dichloromethane was found to be disordered over an inversion center; only one orientation is shown. Hydroxyl hydrogens were disordered over two positions, both positions are shown above.

Table 1. Selected bond distances (Å) and angles (°) in the structure of H₂[OO]^{tBu}

Selected bond distances	
O1-C1 1.451(2)	C10-C11 1.408(2)
C1-C2 1.591(3)	C11-C12 1.387(3)
C1-C6 1.591(3)	C12-C13 1.371(3)

C1-C10 1.586(2)	C13-C14 1.380(3)	
C15-C10 1.511(2)	C14-C15 1.393(2)	
,	C15-C10 1.426(2)	
Selected bond angles		
O1-C1-C10 104.99(13)	C1-C10-C11 113.90(15)	
O1-C1-C2 104.30(13)	C1-C10-C15 130.84(15)	
O1-C1-C6 104.28(13)	C16-C15-C10 119.01(16)	
C10-C1-C2 108.49(14)	C16-C15-C14 110.28(15)	
,	,	
Selected torsion angles		
C14-C15-C16-C1 84.3(2)	C14-C15-C16-C18 86.4(2)	
C10-C15-C16-C17 96.7(2)	C10-C15-C16-C18 -92.7(2)	

3. Supramolecular structure

 $H_2[OO]^{tBu}$ forms one-dimensional polymer chain held together by hydrogen bonding between two consecutive molecules. Two parallel chains are shown in **Figure 4**. This chain-like structure results from the "anti-anti" conformation of $H_2[OO]^{tBu}$ in which both hydroxyls are pointing outward and thus can H-bond with neighboring molecules. The H-bond distance (indicated by the light blue dashed lines in **Figure 4**) is 2.13 Å. It is also noted that due to the inversion center present within the molecule, the hydroxyl hydrogens are disordered over two positions. As the diffraction data was of adequate quality, we were able to locate both hydrogen positions in the difference map. The corresponding O-H bonds are very similar, 0.93(2) and 0.94(2) Å. Only one of these hydrogens participates in the H-bonding network (alternating conformations for the consecutive molecules);. The solvent molecules are positioned above and below the chains.

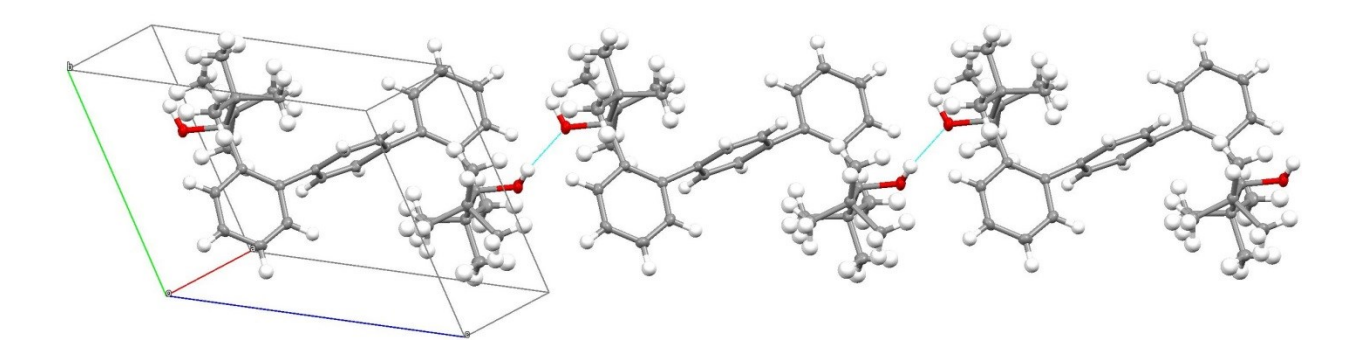


Figure 4. Chain of the H₂[OO]^{tBu} molecules, bridged by H-bonds (indicated in light blue).

4. Database survey.

 $H_2[OO]^{tBu}$ is a new compound that has not been previously synthesized and structurally characterized. As described above, synthesis, structure, and coordination chemistry of the related compound $H_2[OO]^{Ph}$ has been previously reported by us.(Kurup *et al.*, 2019) We note that Agapie and coworkers has previously investigated structurally related 2,2"-diphosphine-1,1':4',1"-terphenyl ligands,(Bailey & Agapie, 2021; Buss *et al.*, 2017) and Fortier and coworkers has investigated structurally related 2,2"-diamide-1,1':4',1"-terphenyl ligands.(Fortier *et al.*, 2017; Yadav *et al.*, 2020) In contrast to $H_2[OO]^{tBu}$, both the diphosphine and the diamide terphenyl ligands served as chelates for the transition metals, adopting *syn* geometry of the phosphine/amide donors relative to the central phenyl.

5. Synthesis and Crystallization

2,2"-dibromo-1,1':4',1"-terphenyl(Velian *et al.*, 2010) (1.00 g, 2.5 mmol) was dissolved in 30 mL THF and cooled under -35 °C. To the cold solution ^tBuLi (1.7 M in pentane, 6.4 mL, 10.8 mmol) was added dropwise and the resulting solution was stirred for 4 h. This reaction mixture was then transferred to a round bottom flask containing hexamethylacetone (8.7 ml, 5 mmol) in

20 mL of hexane and stirred for 24 h. The organic contents were extracted using dichloromethane-water solvent system. The organic phase was dried over MgSO₄ and filtered. The filtrate was concentrated using a rotatory evaporator. The desired product H₂[OO]'Bu was separated in 35% yield (0.464 g, 0.9 mmol) by column chromatography on silica gel using 3% ethyl acetate in hexane. *Para*-terphenyl (1,1':4',1"-terphenyl) was found to be a major byproduct (38% yield, 0.504 g, 2.2 mmol). Purified H₂[OO]'Bu was recrystallized from dichloromethane at -35 °C to obtain colorless crystals suitable for X-ray crystallography. ¹H NMR (25 °C, 400 MHz, CD₂Cl₂) δ 1.05 (s, 25H, CH₃), 1.03 (s, 11H, CH₃), 2.07 (s, 1H, OH), 2.09 (s, 1H, OH), 6.89 (d, *J* = 6.9 Hz, 1H, *ortho*-H), 6.96 (d, *J* = 7.5 Hz, 1H, *ortho*-H), 7.19 (t, *J* = 8.7 Hz, 2H, para-H), 7.33 (m, 6H), 8.28 (d, *J* = 8.2 Hz, 2H, *ortho*-H). ¹³C NMR (25 °C, 125 MHz, CD₂Cl₂) δ 29.99, 30.28, 65.61, 87.36, 125.15, 126.08, 129.47, 130.19, 130.92, 131.37, 134.40, 134.84, 140.76, 144.07, 146.32. HRMS (m/z): Calcd [M-H]⁺ 515.39, found 515.36.

6. Refinement

The structure of H₂[OO]'Bu was collected on a Bruker X8 APEX-II diffractometer with MoKα radiation and a graphite monochromator. The diffraction intensities were measured using a Bruker APEX-II CCD detector. Data were acquired at 100 K with an Oxford 800 Cryostream low-temperature apparatus. The data were processed using APEX3 software supplied by Bruker AXS. The structures were solved by Intrinsic Phasing using SHELXT(Sheldrick 2015a) and refined with SHELXL-2018 (Sheldrick 2015b) using Olex2 (Dolomanov 2009). Hydrogen atoms were placed in calculated positions using a standard riding model and refined isotropically (with the exception of hydroxyl hydrogens); all other atoms were refined anisotropically. The hydroxyl hydrogens were found to be disordered (due to the inversion center located at the H-bond to the adjacent H₂[OO]^{tBu}) over two positions. Two alternating positions were identified

from the Fourier difference maps and refined to 50% occupancy. The CH₂Cl₂ solvent was also disordered by symmetry over two positions and refined with 50% occupancy. Crystal data, data collection, and structure refinement details are summarized in **Table 2** below.

Table 2. Selected bond distances (Å) and angles (°) in the structure of $H_2[OO]^{tBu}$

H ₂ [OO]'Bu Crystal data CagH ₅₀ O ₂ *CH ₂ Cl ₂ M_r 599.68 Crystal system, space group Triclinic, P -1 Temperature (K) 100 a, b, c (Å) 8.2449(4), 9.1248(4), 12.1825(6) a, β, γ (°) 101.530(2), 102.729(3), 109.200(2), 109		
$\begin{array}{cccccccccccccccccccccccccccccccccccc$		H ₂ [OO]'Bu
	Crystal data	
Crystal system, space group Triclinic, P -1 Temperature (K) 100 8.2449(4), 9.1248(4), 12.1825(6) 101.530(2), 102.729(3), 109.200(2), $V(\tilde{A}^3)$ 806.53(7) Z 1 Radiation type Mo K α 9.233 Crystal size (mm) 0.233 0.15×0.1×0.04 Data collection Diffractometer Bruker APEX-II CCD Absorbtion correction Multi-scan (Blessing, 1995) T_{\min}, T_{\max} 0.7215, 0.7455 No. of measured, independent and observed [I > 27197, 3559, 2769 $2\sigma(I)$] reflections R_{int} 0.0365 (sin θ/λ) _{max} (\tilde{A}^{-1}) 0.0513, 0.1246, 1.044 No. of reflections 70.0 of parameters 11 Mixture of independent and constrained refinement Mixture of independent and constrained refinement	Chemical formula	$C_{36}H_{50}O_2*CH_2Cl_2$
Temperature (K) a, b, c (Å) $8.2449(4), 9.1248(4), 12.1825(6)$ $a, β, γ$ (°) $101.530(2), 102.729(3), 109.200(2), V$ (ų) $806.53(7)$ Z 1 Radiation type μ (mm $^{-1}$) 0.233 $0.15 \times 0.1 \times 0.04$ Data collection Diffractometer $0.15 \times 0.1 \times 0.04$ Bruker APEX-II CCD Absorbtion correction $0.15 \times 0.1 \times 0.04$ Multi-scan (Blessing, 1995) $0.7215, 0.7455$ No. of measured, independent and observed [I > 27197, 3559, 2769 $2\sigma(1)$] reflections 0.0365 0.0365 0.0365 0.0365 0.044 Refinement 0.0365 $0.0513, 0.1246, 1.044$ No. of reflections $0.0365 \times 0.0513, 0.1246, 1.044$ No. of reflections $0.0365 \times 0.0513, 0.1246, 1.044$ No. of parameters $0.0365 \times 0.0513, 0.1246, 1.044$	$M_{ m r}$	599.68
$\begin{array}{cccccccccccccccccccccccccccccccccccc$	Crystal system, space group	Triclinic, <i>P</i> -1
$\begin{array}{cccccccccccccccccccccccccccccccccccc$	Temperature (K)	100
$α, β, γ$ (°) $101.530(2), 102.729(3), 109.200(2), V(Å^3)$ $806.53(7)$ Z 1 $Radiation type Mo Kα 0.233 0.15×0.1×0.04 0.233 0.15×0.1×0.04 0.233 0.15×0.1×0.04 0.233 0.15×0.1×0.04 0.233 0.15×0.1×0.04 0.233 0.15×0.1×0.04 0.233 0.15×0.1×0.04 0.15×0.1×0.0$	a, b, c (Å)	8.2449(4), 9.1248(4),
$V(\mathring{A}^3) \qquad 109.200(2), \\ 806.53(7) \\ Z \qquad 1 \\ Radiation type \qquad Mo K\alpha \\ \mu (mm^{-1}) \qquad 0.233 \\ Crystal size (mm) \qquad 0.15\times0.1\times0.04$ $Data collection \\ Diffractometer \qquad Bruker APEX-II CCD \\ Absorbtion correction \qquad Multi-scan (Blessing, 1995) \\ T_{min}, T_{max} \qquad 0.7215, 0.7455 \\ No. of measured, independent and observed [I > 27197, 3559, 2769 \\ 2\sigma(I)] reflections \\ R_{int} \qquad 0.0365 \\ (\sin\theta/\lambda)_{max} (\mathring{A}^{-1}) \qquad 0.644$ $Refinement \\ R[F^2 > 2\sigma(F^2)], wR(F^2), S \qquad 0.0513, 0.1246, 1.044 \\ No. of reflections \qquad 3559 \\ No. of parameters \qquad 211 \\ H-atom treatment \qquad Mixture of independent and constrained refinement$		12.1825(6)
$\begin{array}{cccccccccccccccccccccccccccccccccccc$	α, β, γ (°)	101.530(2), 102.729(3),
$ \begin{array}{cccccccccccccccccccccccccccccccccccc$		109.200(2),
$ \begin{array}{cccccccccccccccccccccccccccccccccccc$	$V(\text{Å}^3)$	806.53(7)
$\begin{array}{llllllllllllllllllllllllllllllllllll$		1
Crystal size (mm) $0.15\times0.1\times0.04$ Data collection Diffractometer Bruker APEX-II CCD Absorbtion correction Multi-scan (Blessing, 1995) $T_{\min}, T_{\max} \qquad 0.7215, 0.7455$ No. of measured, independent and observed [I > 27197, 3559, 2769 $2\sigma(I)] \text{ reflections } R_{\inf} \qquad 0.0365 \\ (\sin\theta/\lambda)_{\max} (\mathring{A}^{-1}) \qquad 0.644$ Refinement $R[F^2 > 2\sigma(F^2)], wR(F^2), S \qquad 0.0513, 0.1246, 1.044$ No. of reflections 3559 No. of parameters 211 H-atom treatment Mixture of independent and constrained refinement	Radiation type	Μο Κα
Data collection Diffractometer Absorbtion correction T_{\min} , T_{\max} No. of measured, independent and observed [I > 27197, 3559, 2769 $2\sigma(I)$] reflections R_{\inf} $\sin(A^{-1})$ Refinement $R[F^2 > 2\sigma(F^2)]$, $wR(F^2)$, S No. of parameters No. of parameters H-atom treatment M_{\max} M_{\min} M	$\mu (\text{mm}^{-1})$	0.233
Diffractometer Bruker APEX-II CCD Multi-scan (Blessing, 1995) T_{\min} , T_{\max} 0.7215, 0.7455 No. of measured, independent and observed [I > 27197, 3559, 2769 $2\sigma(I)$] reflections R_{\inf} 0.0365 $(\sin\theta/\lambda)_{\max}$ (Å $^{-1}$) 0.644 Refinement $R[F^2 > 2\sigma(F^2)]$, $wR(F^2)$, S 0.0513, 0.1246, 1.044 No. of reflections 3559 No. of parameters 211 H-atom treatment Mixture of independent and constrained refinement	Crystal size (mm)	$0.15 \times 0.1 \times 0.04$
Diffractometer Bruker APEX-II CCD Multi-scan (Blessing, 1995) T_{\min} , T_{\max} 0.7215, 0.7455 No. of measured, independent and observed [I > 27197, 3559, 2769 $2\sigma(I)$] reflections R_{\inf} 0.0365 $(\sin\theta/\lambda)_{\max}$ (Å $^{-1}$) 0.644 Refinement $R[F^2 > 2\sigma(F^2)]$, $wR(F^2)$, S 0.0513, 0.1246, 1.044 No. of reflections 3559 No. of parameters 211 H-atom treatment Mixture of independent and constrained refinement	Data collection	
Absorbtion correction Multi-scan (Blessing, 1995) $T_{\min}, T_{\max} \qquad 0.7215, 0.7455$ No. of measured, independent and observed [I > 27197, 3559, 2769 $2\sigma(I)$] reflections $R_{\inf} \qquad 0.0365 \\ (\sin\theta/\lambda)_{\max} (\mathring{A}^{-1}) \qquad 0.644$ Refinement $R[F^2 > 2\sigma(F^2)], wR(F^2), S \qquad 0.0513, 0.1246, 1.044$ No. of reflections 3559 No. of parameters 211 H-atom treatment Mixture of independent and constrained refinement		Bruker APEX-II CCD
$T_{\min}, T_{\max} \\ \text{No. of measured, independent and observed } [I > 27197, 3559, 2769] \\ 2\sigma(I)] \text{ reflections } \\ R_{\text{int}} \\ (\sin\theta/\lambda)_{\text{max}} (\mathring{A}^{-1}) \\ \text{Refinement } \\ R[F^2 > 2\sigma(F^2)], wR(F^2), S \\ \text{No. of reflections } \\ \text{No. of parameters } \\ \text{H-atom treatment } \\ \text{H-atom treatment } \\ \text{Mixture of independent and constrained refinement } \\ \text{No. of reflections } \\ \text{Mixture of independent and constrained refinement } \\ No. of the problem of the probl$		
T_{\min} , T_{\max} 0.7215, 0.7455 No. of measured, independent and observed [I > 27197, 3559, 2769 $2\sigma(I)$] reflections 0.0365 $(\sin\theta/\lambda)_{\max}$ (Å ⁻¹) 0.044 Refinement $R[F^2 > 2\sigma(F^2)]$, $wR(F^2)$, S 0.0513, 0.1246, 1.044 No. of reflections 3559 No. of parameters 211 H-atom treatment Mixture of independent and constrained refinement		, , , , , , , , , , , , , , , , , , , ,
No. of measured, independent and observed $[I > 27197, 3559, 2769 2\sigma(I)]$ reflections $R_{\rm int}$ 0.0365 $(\sin\theta/\lambda)_{\rm max}({\rm Å}^{-1})$ 0.644 $ Refinement \\ R[F^2 > 2\sigma(F^2)], wR(F^2), S \\ No. of reflections \\ No. of parameters \\ H-atom treatment \\ Mixture of independent and constrained refinement $	T_{\min} , T_{\max}	,
$\begin{array}{cccccccccccccccccccccccccccccccccccc$		· ·
R_{int} 0.0365 ($\sin \theta/\lambda$) $_{\text{max}}$ (Å $^{-1}$) 0.644 Refinement $R[F^2 > 2\sigma(F^2)], wR(F^2), S$ 0.0513, 0.1246, 1.044 No. of reflections 3559 211 H-atom treatment Mixture of independent and constrained refinement	-	, ,
$\begin{array}{lll} (\sin\theta/\lambda)_{\max} (\mathring{A}^{-1}) & 0.644 \\ \\ \text{Refinement} & & \\ R[F^2 > 2\sigma(F^2)], wR(F^2), S & 0.0513, 0.1246, 1.044 \\ \text{No. of reflections} & 3559 \\ \text{No. of parameters} & 211 \\ \text{H-atom treatment} & \text{Mixture of independent} \\ & & \text{and} & \text{constrained} \\ & & & \text{refinement} \end{array}$	\ \frac{1}{2}	0.0365
Refinement $R[F^2 > 2\sigma(F^2)]$, $wR(F^2)$, S 0.0513, 0.1246, 1.044 No. of reflections 3559 No. of parameters 211 H-atom treatment Mixture of independent and constrained refinement		0.644
$R[F^2 > 2\sigma(F^2)], wR(F^2), S$ 0.0513, 0.1246, 1.044 No. of reflections 3559 No. of parameters 211 H-atom treatment Mixture of independent and constrained refinement	(*************************************	
No. of reflections No. of parameters H-atom treatment Mixture of independent and constrained refinement		
No. of parameters H-atom treatment Mixture of independent and constrained refinement	$R[F^2 > 2\sigma(F^2)], wR(F^2), S$	0.0513, 0.1246, 1.044
H-atom treatment Mixture of independent and constrained refinement	No. of reflections	3559
and constrained refinement	No. of parameters	211
and constrained refinement	H-atom treatment	Mixture of independent
$\Delta \rho_{\text{max}}, \Delta \rho_{\text{min}} (e \text{ Å}^{-3})$ 0.570, -0.430		refinement
	$\Delta \rho_{\text{max}}, \Delta \rho_{\text{min}}$ (e Å ⁻³)	0.570, -0.430

Computer programs: APEX3 and SAINT (Bruker, 2016), SHELXT (Sheldrick 2015a), SHELXL-2018/3 (Sheldrick, 2015b), and Olex2 (Dolomanov 2009).

Funding

S. G. is grateful to the National Science Foundation for current support under grant number CHE-1855681.

References

Bailey, G. A. & Agapie, T. (2021). Organometallics 40, 16, 2881-2887.

Bellow, J. A., Stoian, S. A., Van Tol, J., Ozarowski, A., Lord, R. L. & Groysman, S. (2016). *J. Am. Chem. Soc.* (138) 5531-5534.

Bellow, J. A., Yousif, M., Cabelof, A. C., Lord, R. L. & Groysman, S. (2015). *Organometallics* **34**, 2917-2923

Bellow, J. A., Yousif, M. & Groysman, S. (2016). Comments Inorg. Chem. 36, 92-122.

Blessing, R. H. (1995). Acta Cryst. A51, 33-38.

Buss, J. A., Oyala, P. H. & Agapie, T. (2017). Angew. Chem. Int. Ed. 56, 14502-14506.

Brazeau, S. E. N. & Doerrer, L. H. (2019). Dalton Trans. 48, 6899-6909.

Chua, Y.-Y. & Duong, H. A. (2014). Chem. Commun. 50, 8424-8427.

Dolomanov, O.V., Bourhis, L.J., Gildea, R.J, Howard, J.A.K. & Puschmann, H. (2009). *J. Appl. Cryst.* **42**, 339-341.

Fortier, S.; Aguilar-Calderón, J. R., Vlaisavljevich, B., Metta-Magaña, A. J., Goos, A. G. & Botez, C. E. (2017). *Organometallics* **36**, 4591–4599.

Grass, A., Dewey. N. S., Lord, R. L. & Groysman, S. (2019). Organometallics 38, 962-972.

Grass, A.; Bellow, J. A.; Morrison, G.; zur Loye, H.-C.; Lord, R. L. & Groysman, S. (2020). *Chem. Commun.* **56**, 8416-8419.

Grass, A., Wannipurage, D., Lord, R. L. & Groysman, S. (2019). Coord. Chem. Rev. 400, 1-16.

Hannigan, S. F, Arnoff, A. I., Neville, S. E., Lum, J. S., Golen, J. A., Rheingold, A. L., Nicole Orth, N., Ivanović-Burmazović, I., Liebhäuser, P., Rösener, T., Stanek, J., Hoffmann, A., Herres-Pawlis, S. & Doerrer, L. H. (2017). *Chem. Eur. J.* 23, 8212-8224.

Jayasundara, C. R. K., Sabasovs, D., Staples, R. J., Oppenheimer, J., Smith, M. R., III & Maleczka, R. E., Jr. (2018). *Organometallics* 37, 1567–1574.

Kurup, S. S., Staples, R. J., Lord, R. L. & Groysman, S. (2020). Molecules 25, 373.

Kurup, S. S., Wannipurage, D., Lord, R. L. & Groysman, S. (2019). Chem. Commun. 55, 10780-10783.

Sheldrick, G.M. (2015a). Acta Cryst. A71, 3-8.

Sheldrick, G.M. (2015b). Acta Cryst. C71, 3-8.

Velian, A. Lin, S. Miller, A. J. M. Day, M. W. & Agapie, T, J. (2010). J. Am. Chem. Soc. 132, 6296-6297
Wannipurage, D., Hollingsworth, T. S., Santulli, F., Cozzolino, M., Lamberti, M., Groysman, S. & Mazzeo, M. (2020). Dalton Trans. 2715-2723.

Wannipurage, D., Kurup, S. S. & Groysman, S. (2021). Organometallics 40, 3637–3644.

Yadav, M., Metta-Magaña, A. & Fortier, S. (2020). Chem. Sci. 11, 2381-2387.

Yousif, M., Wannipurage, D., Huizenga, C. D., Washnock-Schmid, E., Peraino, N. J., Ozarowski, A., Stoian, S. A., Lord, R. L. & Groysman, S. (2018). *Inorg. Chem.* 57, 9425-9438.

Yousif, M., Tjapkes, D. J., Lord, R. L. and Groysman, S. (2015). Organometallics 34, 5119 - 5128.